DMD Fast Forward. Published on October 18, 2006 as DOI: 10.1124/dmd.106.012252
DMD Fast Forward. Published on October 18, 2006 as doi:10.1124/dmd.106.012252
This article has not been copyedited and formatted. The final version may differ from this version.

DMD #12252

TITLE PAGE

CYP2B6, CYP2D6 and CYP3A4 catalyse the primary oxidative metabolism of perhexiline enantiomers by human liver microsomes

Benjamin J Davies

Janet K Coller

Andrew A Somogyi

Robert W Milne

Benedetta C Sallustio

Discipline of Pharmacology, School of Medical Sciences, The University of Adelaide, Adelaide, South Australia (B.J.D., J.K.C., A.A.S., B.C.S.)

Department of Cardiology and Clinical Pharmacology, The Queen Elizabeth Hospital, Adelaide, South Australia (B.J.D., B.C.S.)

Sansom Institute, University of South Australia, Adelaide, South Australia (R.W.M.)

Downloaded from dmd.aspetjournals.org at ASPET Journals on April 10, 2024

Copyright 2006 by the American Society for Pharmacology and Experimental Therapeutics.

DMD Fast Forward. Published on October 18, 2006 as DOI: 10.1124/dmd.106.012252
This article has not been copyedited and formatted. The final version may differ from this version.

RUNNING TITLE PAGE

Running Title

CYP2B6, CYP2D6 and CYP3A4 metabolise perhexiline enantiomers

Corresponding Author

Benedetta C Sallustio

Department of Cardiology and Clinical Pharmacology, The Queen Elizabeth Hospital, 28 Woodville Road, Woodville, SA 5011, Australia

Telephone +61 8 8222 6510

Fax +61 8 8222 6033

E-mail benedetta.sallustio@nwahs.sa.gov.au

Number of text pages	45
Number of tables	1
Number of figures	8
Number of references	41
Number of words in the abstract	243
Number of words in the introduction	613
Number of words in the discussion	1912

List of non-standard abbreviations

PHX, perhexiline; HLM, human liver microsomes; EM, extensive metaboliser; IM, intermediate metaboliser; PM, poor metaboliser; UM, ultra-rapid metaboliser; thio-TEPA, triethylenethiophosphoramide; MAB, monoclonal antibody; HPLC, high-

Downloaded from dmd.aspetjournals.org at ASPET Journals on April 10, 2024

DMD Fast Forward. Published on October 18, 2006 as DOI: 10.1124/dmd.106.012252
This article has not been copyedited and formatted. The final version may differ from this version.

performance liquid chromatography; $f_{u(mic)}$, unbound fraction in the microsomal compartment; C_B, bound drug concentration; C_F, free drug concentration; B_{max}, maximal binding capacity; K_D, equilibrium dissociation constant; C_T, total drug concentration; K_m, Michaelis-Menten constant; V_{max}, maximal reaction rate; V, reaction rate; S, free substrate concentration; K_s, substrate inhibitor constant; Cl_{int}, intrinsic clearance

Downloaded from dmd.aspetjournals.org at ASPET Journals on April 10, 2024

DMD Fast Forward. Published on October 18, 2006 as DOI: 10.1124/dmd.106.012252
This article has not been copyedited and formatted. The final version may differ from this version.

ABSTRACT

The cytochrome P450 (CYP)-mediated 4-monohydroxylations of the individual enantiomers of the racemic anti-anginal agent perhexiline (PHX) were investigated in human liver microsomes (HLM) to identify stereoselective differences in metabolism and to determine the contribution of the polymorphic enzyme CYP2D6 and other CYPs to the intrinsic clearance of each enantiomer. The *cis*-, *trans1*- and *trans2*-4-monohydroxylation rates of (+)- and (-)-PHX by human liver microsomes from three extensive (EM), two intermediate (IM) and two poor (PM) CYP2D6 metabolisers were measured with a high-performance liquid chromatography (HPLC) assay. CYP isoform-specific inhibitors, monoclonal antibodies directed against CYP isoforms and recombinant expressed human CYP enzymes were used to define the CYP isoform profile of PHX 4-monohydroxylations. The total *in vitro* intrinsic clearance (mean ± SD) of (+)-and (-)-PHX was 1376 ± 330 and 2475 ± 321, 230 ± 225 and 482 ± 437, and 63.4 ± 1.6 and 54.6 ± 1.2 μl/min/mg for the EM, IM and PM HLM, respectively. CYP2D6 catalyses the formation of *cis*-OH-(+)-PHX and *trans1*-OH-(+)-PHX from (+)-PHX and *cis*-OH-(-)-PHX from (-)-PHX with high affinity. CYP2B6 and CYP3A4 each catalyse the *trans1*- and *trans2*-4-monohydroxylation of both (+)- and (-)-PHX with low affinity. Both enantiomers of PHX are subject to significant polymorphic metabolism by CYP2D6, although this enzyme exhibits distinct stereoselectivity with respect to the conformation of metabolites and the rate at which they are formed. CYP2B6 and CYP3A4 are minor contributors to the intrinsic CYP-mediated hepatic clearance of both enantiomers of PHX, except in CYP2D6 PM.

Downloaded from dmd.aspetjournals.org at ASPET Journals on April 10, 2024

DMD Fast Forward. Published on October 18, 2006 as DOI: 10.1124/dmd.106.012252
This article has not been copyedited and formatted. The final version may differ from this version.

Perhexiline (2-(2,2-dicyclohexylethyl)piperidine, PHX) produces significant incremental antianginal effects in patients with intractable angina who are unsuitable for surgical treatment and intolerant or refractory to maximal antianginal therapy (Cole et al., 1990). Its use is limited by the potential to cause severe hepatotoxicity and peripheral neuropathy associated with elevated plasma PHX concentrations (Morgan et al., 1984, Shah et al., 1982), although the risk of toxicity is significantly reduced by maintaining total plasma PHX concentrations between 0.15 and 0.60 mg/l (0.54 to 2.16 μM) (Cole et al., 1990). The confounding factor in treatment with PHX is its dependence on the polymorphic cytochrome P450 2D6 (CYP2D6) isoform for hepatic *cis*-4-monohydroxylation (Cooper et al., 1984) as the principal determinant of clearance (Sallustio et al., 2002), resulting in extreme interindividual pharmacokinetic variability. CYP2D6 poor metabolisers (PM) are typically maintained within the therapeutic range with a dose of approximately 100 mg of PHX maleate per week, whereas intermediate (IM), extensive (EM) and ultra-rapid metabolisers (UM) require doses of 100 to 500 mg per day to achieve similar concentrations in plasma (Sallustio et al., 2002).

An investigation of the *in vitro* enzyme kinetics of PHX 4-monohydroxylation in human liver microsomes (HLM) determined that it is almost exclusively catalysed with high affinity by CYP2D6 in EM, with K_m values within the range of therapeutic PHX concentrations in plasma (Sørensen et al., 2003); this is consistent with the non-linear kinetics observed clinically in EM (Cooper et al., 1985). The intrinsic clearance of PHX was approximately 100-fold lower in PM, presumably mediated by CYP isoforms other than CYP2D6 with a much lower affinity for PHX (Sørensen et al.,

Downloaded from dmd.aspetjournals.org at ASPET Journals on April 10, 2024

DMD Fast Forward. Published on October 18, 2006 as DOI: 10.1124/dmd.106.012252
This article has not been copyedited and formatted. The final version may differ from this version.

2003), although these isoforms and the 4-monohydroxy metabolites they produced were not identified.

PHX is formulated as a racemic mixture of (+) and (-) enantiomers (Pexsig®, Sigma Pharmaceuticals, Clayton, Victoria, Australia) and six 4-monohydroxy metabolites are possible, being composed of one pair each of *cis*-, *trans1*- and *trans2*-4-monohydroxy PHX enantiomers (Figure 1) that co-elute chromatographically (Davies et al., in press), although their absolute configurations are unknown. Gould et al. (1986) were the first to investigate the pharmacokinetics of the individual enantiomers of PHX. Single 300 mg oral doses of either (+)- or (-)-PHX were administered to eight EM. The oral clearance of the PHX enantiomer and the AUC of the corresponding CYP2D6-dependent *cis*-4-monohydroxy metabolite was 2.5- and 28-fold greater, respectively, following administration of (-)- than (+)-PHX. Whereas (+)-PHX was metabolised to *cis*-OH-(+)-PHX and *trans1*-OH-(+)-PHX at similar rates, (-)-PHX displayed distinct stereoselective metabolism to *cis*-OH-(-)-PHX. Thus, the authors suggested that (+)-PHX may display a smaller polymorphic effect in its metabolism. A recent investigation into the effect of CYP2D6 on the *in vivo* disposition of the enantiomers of PHX by this laboratory (Inglis et al., in press) concluded that both enantiomers display significant polymorphic and saturable metabolism by CYP2D6. Among EM patients, the median oral clearance of (-)-PHX was 1.4-fold greater than that of (+)-PHX, attributable to enantioselective metabolism by CYP2D6. Interestingly, PM patients demonstrated greater enantioselectivity in the oral clearance of (-)- versus (+)-PHX, with a median ratio of 2.3, although the mechanism responsible is unknown.

Downloaded from dmd.aspetjournals.org at ASPET Journals on April 10, 2024

DMD Fast Forward. Published on October 18, 2006 as DOI: 10.1124/dmd.106.012252
This article has not been copyedited and formatted. The final version may differ from this version.

To date, chiral analytical methods capable of resolving the 4-monohydroxy metabolites of racemic PHX with sufficient sensitivity for pharmacokinetic studies have not been reported. However, this laboratory recently developed an achiral method (Davies et al., in press) which is suitable for characterising the 4-monohydroxy metabolites of the individual enantiomers of PHX. The current study was undertaken to determine the *in vitro* kinetics of the formation of the 4-monohydroxy metabolites of (+)- and (-)-PHX in human liver microsomes from CYP2D6 EM, IM and PM, to characterise the CYP isoform profile of these metabolic pathways and to describe any stereochemical differences in metabolism.

Downloaded from dmd.aspetjournals.org at ASPET Journals on April 10, 2024

DMD Fast Forward. Published on October 18, 2006 as DOI: 10.1124/dmd.106.012252
This article has not been copyedited and formatted. The final version may differ from this version.

METHODS

Materials

(+)- and (-)-PHX HCl were prepared according to the method described by Davies et al. (2006a). The *cis*-OH-(±)-PHX reference compound was supplied by Marion Merrell Dow (Kansas City, KS, USA). The *trans1*- and *trans2*-OH-(±)-PHX reference compounds were supplied by Sigma Pharmaceuticals (South Croydon, VIC, Australia). Furafylline and *S*-mephenytoin were purchased from Ultrafine Chemicals (Manchester, England). Diethyldithiocarbamate, (±)-isocitric acid Na_3, isocitrate dehydrogenase (NADP, type IV), sulphaphenazole, troleandomycin and coumarin were purchased from Sigma Chemical Company (St Louis, MO, USA). Quinidine sulphate and nicotinamide dinucleotide phosphate sodium salt were purchased from Merck (Darmstadt, Germany). Triethylenethiophosphoramide (thio-TEPA) was purchased from Sigma Pharmaceuticals (South Croydon, VIC, Australia). Monoclonal antibodies raised against human CYP1A2 (MAB-1A2), CYP2D6 (MAB-2D6), CYP2E1 (MAB-2E1) and CYP3A4 (MAB-3A4) and microsomes from human lymphoblastoid cells containing recombinant expressed CYP2C19, CYP2D6, CYP3A4 or the expression vector without *CYP* cDNA (control microsomes) were purchased from BD GENTEST^{TM} (a BD Biosciences Company, Woburn. MA, USA). Recombinant expressed and purified CYP2B6 from DH5α strain *Escherichia coli* (Notley et al., 2002) was a gift of Dr Elizabeth Gillam (Department of Physiology and Pharmacology, School of Biomedical Sciences, University of Queensland, St Lucia, Australia). A monoclonal antibody raised against human CYP2B6 (MAB-2B6) was

Downloaded from dmd.aspetjournals.org at ASPET Journals on April 10, 2024

DMD Fast Forward. Published on October 18, 2006 as DOI: 10.1124/dmd.106.012252
This article has not been copyedited and formatted. The final version may differ from this version.

purchased from Invitrogen Corporation (Carlsbad, CA, USA). All other reagents and chemicals were obtained from commercial sources and were of analytical grade.

Human liver microsomes

Ethics approval was obtained from the Human Ethics Committee of the Royal Adelaide Hospital to obtain human liver samples (n=7) during partial hepatectomy from patients who had given written informed consent for their tissue to be used, as previously reported (Hutchinson et al., 2004). Samples were stored at -80°C. The donors all had normal clinical chemistry and haematology measurements prior to surgery and all the tissue samples used were normal based on gross morphology. HLM #18, 21, 24, 31, 36, 39 and 46 (internal code) were prepared by differential centrifugation of liver homogenates and were stored in buffer at -80°C until use (Zanger et al., 1988). The total protein concentration (Lowry et al., 1951) of the HLM preparations ranged from 17.0 to 32.7 mg/ml and the total CYP concentration (Omura and Sato, 1964) ranged from 202 to 437 pmol/mg microsomal protein.

Genomic DNA was isolated from liver tissue samples using a QIAamp® DNA mini kit, according to the manufacturer's protocol (QIAGEN Pty Ltd, Clifton Hill, Australia). *CYP2D6* genotyping was performed as previously reported (James et al., 2004, Davies et al., 2006b). HLM# 21, 31 and 46 each carried two functional *CYP2D6* alleles (genotypes of *CYP2D6*1/*1*, **1/*41* and **1/*2D*, respectively) and were classified as EM. HLM# 18 and 36 each carried one functional *CYP2D6* allele (genotypes of *CYP2D6*1/*4* and **2J/*4*, respectively) and were classified as IM.

Downloaded from dmd.aspetjournals.org at ASPET Journals on April 10, 2024

DMD Fast Forward. Published on October 18, 2006 as DOI: 10.1124/dmd.106.012252
This article has not been copyedited and formatted. The final version may differ from this version.

HLM# 24 and 39 carried no functional *CYP2D6* alleles (genotypes of *CYP2D6*4/*4*) and were classified as PM.

Microsomal incubations

Microsomal incubations were linear with time up to 60 min and with protein concentrations up to 1.0 mg/ml with respect to *cis*-, *trans1*- and *trans2*-4-monohydroxylation of (+)- or (-)-PHX at total concentrations of 0.1-100 μM. Accordingly, microsomal incubations were performed in triplicate at 37°C in a shaking water bath for 30 min in 0.1 M phosphate buffer (pH 7.4) containing HLM protein (0.25 mg/ml), (+)- or (-)-PHX HCl (0.1-100 μM, added as a stock dissolved in methanol to produce a final methanol concentration of 0.5% v/v) and an NADPH generating system composed of 1 mM NADP, 5 mM isocitrate, 1 U/ml isocitrate dehydrogenase type IV and 5 mM $MgCl_2$. The incubations were stopped by rapid cooling on ice.

HPLC assay of the 4-monohydroxy metabolites of (+)- and (-)-PHX

The formation of *cis*-, *trans1*- and *trans2*-OH-(+)-PHX from (+)-PHX and *cis*-, *trans1*- and *trans2*-OH-(-)-PHX from (-)-PHX in microsomal incubations was determined using a recently developed method (Davies et al., in press). The inter-assay (n=31) CV and bias were <10% and <5%, respectively, for the 0.4 mg/l QC samples, <15% and <10%, respectively, for the 0.075 mg/l QC samples, and <15% for both CV and bias for the 0.015 mg/l QC samples. There was no chromatographic interference with any of the peaks of interest from endogenous compounds in HLM,

Downloaded from dmd.aspetjournals.org at ASPET Journals on April 10, 2024

DMD Fast Forward. Published on October 18, 2006 as DOI: 10.1124/dmd.106.012252
This article has not been copyedited and formatted. The final version may differ from this version.

the NADPH generating system, putative chemical inhibitors, monoclonal antibodies or human lymphoblastoid cells containing recombinant expressed CYPs (data not shown).

Non-specific binding of (+)- and (-)-perhexiline in microsomal incubations

The non-specific binding of (+)- and (-)-PHX to HLM was determined by equilibrium dialysis using dialysis cells of 4.5 ml capacity per side and Spectra/Por® #4 dialysis membrane with a molecular weight cut off of 12 to 14 kDa, purchased from Spectrum Medical Industries Inc. (Los Angeles, CA, USA). The sample volume on each side of the cell was 4 ml. The dialysis membrane was prepared according to the manufacturer's instructions. Equilibrium dialysis was performed for 16 h at 37 °C according to the method of McLure et al. (2000), except the microsomal protein concentration was the same as for the microsomal incubations (0.25 mg/ml), final total (+)- or (-)-PHX concentrations were in the range of 1 to 100 μM (added as a stock dissolved in methanol to produce a final methanol concentration of 0.5% v/v), and high and low concentration controls used to establish the 16 h dialysis time necessary to attain equilibrium contained 100 and 5 μM, respectively, of (+)- or (-)-PHX. Following dialysis, total and free (+)- and (-)-PHX concentrations were determined by HPLC (Davies et al., 2006a). Standard curves for microsomes and buffer were linear with r^2 values of 0.995 to 0.999. Triplicate determinations of three concentration points in the standard curves and of all samples produced coefficients of variation <10%.

Downloaded from dmd.aspetjournals.org at ASPET Journals on April 10, 2024

DMD Fast Forward. Published on October 18, 2006 as DOI: 10.1124/dmd.106.012252
This article has not been copyedited and formatted. The final version may differ from this version.

For each dialysis cell the unbound fraction of (+)- or (-)-PHX in the microsomal compartment ($f_{u(mic)}$) was calculated as the free drug concentration (concentration in the buffer compartment) divided by the total drug concentration (concentration in the microsomal compartment). These values were entered into iterative unweighted non-linear least-squares regression analyses using GraphPad Prism v4.02 (GraphPad Software Inc., San Diego, CA, USA) for

$$C_B = (B_{max} \,.\, C_F) / (K_D + C_F) \qquad \text{equation (1)}$$

where C_B is the concentration of drug bound, C_F is the free drug concentration, B_{max} is the maximal binding capacity and K_D is the equilibrium dissociation constant, equivalent to the free drug concentration at which binding is half of its maximum.

Kinetic analyses of (+)- and (-)-PHX metabolism in microsomal incubations

To simulate the effects of non-specific binding on *in vitro* kinetics, the free (+)- and (-)-PHX concentrations in the microsomal incubations were calculated using the B_{max} and K_D values derived from the non-specific binding study to solve equation (1) for the free substrate concentration (C_F) corresponding to each total substrate concentration (C_T), where $C_B = C_T - C_F$ (McLure et al., 2000).

The rates of *cis*-, *trans1*- and *trans2*-4-monohydroxylation of (+)- and (-)-PHX were expressed as pmol/min/mg microsomal protein. Initial estimates of K_m and V_{max} were obtained from Eadie Hofstee (V/[S] vs V) plots. These values were entered into iterative unweighted non-linear least-squares regression analyses using GraphPad Prism v4.02 for one and two enzyme Michaelis-Menten models, both with and

Downloaded from dmd.aspetjournals.org at ASPET Journals on April 10, 2024

DMD Fast Forward. Published on October 18, 2006 as DOI: 10.1124/dmd.106.012252
This article has not been copyedited and formatted. The final version may differ from this version.

without simple uncompetitive substrate inhibition (Tracy and Hummel, 2004), as follows:

one enzyme model

$$V = (V_{max} \cdot S) / (K_m + S) \qquad \text{equation (2)}$$

one enzyme model with uncompetitive substrate inhibition

$$V = (V_{max} \cdot S) / [(K_m + S) + (S^2 / K_s)] \qquad \text{equation (3)}$$

two enzyme model

$$V = (V_{max1} \cdot S) / (K_{m1} + S) + (V_{max2} \cdot S) / (K_{m2} + S) \qquad \text{equation (4)}$$

two enzyme model with uncompetitive substrate inhibition

$$V = (V_{max1} \cdot S) / [(K_{m1} + S) + (S^2 / K_{s1})] + (V_{max2} \cdot S) / [(K_{m2} + S) + (S^2 / K_{s2})] \qquad \text{equation (5)}$$

where V is reaction rate, V_{max} is the maximal reaction rate, S is the free substrate concentration (calculated as C_F from equation 1), K_m is the Michaelis-Menten constant, equivalent to the free substrate concentration at which the reaction rate is half of its maximum and K_s is the substrate inhibitor constant, equivalent to the free substrate concentration at which half the V_{max} is inhibited. Models were compared by examination of residuals and extra sum-of-squares F test, with $P<0.05$ considered statistically significant. The intrinsic clearance (Cl_{int}) for each metabolic pathway was calculated as V_{max}/K_m. The mean Cl_{int} for each metabolic pathway was calculated for

Downloaded from dmd.aspetjournals.org at ASPET Journals on April 10, 2024

DMD Fast Forward. Published on October 18, 2006 as DOI: 10.1124/dmd.106.012252
This article has not been copyedited and formatted. The final version may differ from this version.

EM, IM and PM HLM and the total Cl_{int} from the sum of the Cl_{int} for each metabolic pathway.

Chemical inhibition studies

HLM from three *CYP2D6* EM (# 21, 31 and 46) and one *CYP2D6* IM (# 18) were incubated in triplicate with the NADPH regenerating system and a selection of CYP isoform-specific chemical inhibitors. Free substrate concentrations approximated the apparent K_m values estimated for each pathway in each HLM. The CYP isoform-specific chemical inhibitors (Baldwin et al., 1995, Newton et al., 1995, Rae et al., 2002, Tucker et al., 2001) used (CYP isoform and final microsomal incubation concentration) were quinidine (CYP2D6, 1 μM), coumarin (CYP2A6, 100 μM), diethyldithiocarbamate (CYP2E1, 10μM) and thio-TEPA (CYP2B6, 50 μM), each dissolved in water, *S*-mephenytoin (CYP2C19, 100 μM) and troleandomycin (CYP3A4, 10 μM), each dissolved in 0.5% methanol, furafylline (CYP1A2, 100 μM) dissolved in 0.1% acetonitrile, and sulphaphenazole (CYP2C9, 100 μM) dissolved in 0.83% dimethylsulphoxide. Where inhibitor stocks were made using organic solvents, incubations containing equivalent solvent concentrations were used as controls. The incubation conditions were not altered from the kinetic analyses, except that the mechanism-based inhibitors diethyldithiocarbamate, thio-TEPA, furafylline and troleandomycin were preincubated for 20 min at 37°C with all incubation constituents prior to initiating the reaction by adding the substrate. Control incubations were similarly preincubated, but in the absence of the inhibitor.

Downloaded from dmd.aspetjournals.org at ASPET Journals on April 10, 2024

DMD Fast Forward. Published on October 18, 2006 as DOI: 10.1124/dmd.106.012252
This article has not been copyedited and formatted. The final version may differ from this version.

The results of the IM and the three EM HLM were grouped to assess the significance of inhibition using one-way paired t-tests. Statistical significance was set at $P<0.05$ and all the data was expressed as the mean ± standard deviation (SD). Changes in activity of 15% or less from the controls were not considered to be significant. Based upon the interpretation of these results, one PM HLM (# 24) was similarly incubated with the inhibitors quinidine, coumarin, troleandomycin and thio-TEPA.

Inhibition by monoclonal antibodies

HLM from a *CYP2D6* EM (# 31) were incubated in duplicate with the NADPH regenerating system and a selection of monoclonal antibodies directed towards CYP1A2 (MAB-1A2), CYP2B6 (MAB-2B6), CYP2D6 (MAB-2D6), CYP2E1 (MAB-2E1) and CYP3A4 (MAB-3A4). The concentration of antibodies was in accordance with the manufacturers' instructions. Free substrate concentrations approximated the apparent K_m values estimated for each pathway. The incubation conditions were not altered from the kinetic analyses, except that the HLM and antibodies were pre-incubated for 15 min on ice, prior to addition of the remaining incubation constituents. Control incubations were similarly preincubated, but without antibodies. Changes in activity of 15% or less from the controls were not considered to be significant.

Metabolism by recombinant expressed human CYP isoforms

Microsomes containing recombinant expressed human CYP2B6, CYP2C19, CYP2D6, CYP3A4 or the expression vector without *CYP* cDNA were incubated in

Downloaded from dmd.aspetjournals.org at ASPET Journals on April 10, 2024

DMD Fast Forward. Published on October 18, 2006 as DOI: 10.1124/dmd.106.012252
This article has not been copyedited and formatted. The final version may differ from this version.

duplicate with the NADPH regenerating system and 10 μM free (+)- or (-)-PHX to qualitatively determine metabolite formation. Incubation conditions were the same as in the kinetic study, except that the microsomes were kept on ice until added to the reaction mixture. The protein concentration used was the same as in the kinetic studies (0.25 mg/ml).

Metabolism by recombinant expressed human CYP3A4 with 100 μM coumarin

Microsomes containing recombinant expressed human CYP3A4 were incubated in duplicate with the NADPH regenerating system and 1 μM free (+)- or (-)-PHX, with or without coumarin (final coumarin concentration of 100 μM), to detect a change in metabolite formation caused by the presence of coumarin. Incubation conditions were the same as in the kinetic study, except that the microsomes were kept on ice until added to the reaction mixture. The protein concentration used was the same as in the kinetic studies (0.25 mg/ml).

Downloaded from dmd.aspetjournals.org at ASPET Journals on April 10, 2024

DMD Fast Forward. Published on October 18, 2006 as DOI: 10.1124/dmd.106.012252
This article has not been copyedited and formatted. The final version may differ from this version.

RESULTS

Non-specific binding of (+)- and (-)-perhexiline in microsomal incubations

(+)- and (-)-PHX were extensively bound to the microsomal membrane. Binding was saturable, with B_{max} and K_D values (±SE) of 54.6 ± 3.5 and 3.6 ± 0.7 μM, respectively, for (+)-PHX, and 56.3 ± 5.0 and 4.8 ± 1.1 μM, respectively, for (-)-PHX (Figure 2). Over the range of total (+)- and (-)-PHX concentrations used in the HLM studies (0.1 to 100 μM), the $f_{u(mic)}$ ranged from approximately 0.07 to 0.5.

Kinetic analyses

The Eadie-Hofstee plots generally displayed an inflection in the upper quadrant (data not shown), indicative of substrate inhibition, and most of the kinetic data best fitted a model incorporating substrate inhibition (Table 1). All the data best fitted single enzyme models, except for the formation of *trans1*-OH-(+)-PHX by the three EM HLM and one of the IM HLM (# 18). In these instances the Eadie-Hofstee plots were biphasic (data not shown), indicating the involvement of a high affinity and a low affinity process (Table 1B). Representative *cis*-, *trans1*- and *trans2*-4-monohydroxylation formation rates from (+)- or (-)-PHX versus free substrate concentration curves are shown for an EM, IM and PM HLM (Figure 3).

Cis-4-monohydroxylation

Cis-OH-(+)-PHX and *cis*-OH-(-)-PHX concentrations were below the limit of quantification in incubations with PM HLM. For the EM and IM HLM, *cis*-4-

Downloaded from dmd.aspetjournals.org at ASPET Journals on April 10, 2024

DMD Fast Forward. Published on October 18, 2006 as DOI: 10.1124/dmd.106.012252
This article has not been copyedited and formatted. The final version may differ from this version.

monohydroxylation of both PHX enantiomers was mediated by a high affinity enzyme ((+)-PHX: K_m (mean ± SD) 0.060 ± 0.067 μM, range 0.024-0.160 μM, (-)-PHX: K_m 0.057 ± 0.028 μM, range 0.032-0.104 μM), except for the formation of *cis*-OH-(+)-PHX by IM HLM# 36, which was formed with low affinity (K_m 2.5 μM) (Table 1A).

Trans1-4-monohydroxylation

Formation of *trans1*-OH-(+)-PHX was mediated by a high affinity reaction for the EM HLM and the IM HLM# 18 (K_m 0.020 ± 0.004 μM, range 0.015-0.023 μM). A low affinity reaction also catalysed this process in all the HLM (K_m 2.0 ± 0.4 μM, range 1.6-2.7 μM). A single low affinity reaction was indicated in the formation of *trans1*-OH-(-)-PHX, (K_m 2.3 ± 0.6 μM, range 1.8-3.3 μM) (Table 1B).

Trans2-4-monohydroxylation

A single low affinity reaction was indicated in the formation of *trans2*-OH-(+)-PHX (K_m 1.9 ± 0.5 μM, range 1.4-2.6 μM) and *trans2*-OH-(-)-PHX (K_m 2.6 ± 0.7 μM, range 1.8-3.7 μM) (Table 1C) for all HLM.

Intrinsic clearance

The total Cl_{int} (mean ± SD) of (+)-PHX was 1376 ± 330, 230 ± 225 and 63.4 ± 1.6 μl/min/mg for the EM, IM and PM HLM, respectively. Likewise for (-)-PHX, the total Cl_{int} was 2475 ± 321, 482 ± 437 and 54.6 ± 1.2 μl/min/mg, respectively. The mean involvement of each oxidative metabolic pathway for EM, IM and PM HLM is presented in Figure 4. The primary metabolite of (+)-PHX for EM and IM HLM was *trans1*-OH-(+)-PHX, whereas for (-)-PHX it was *cis*-OH-(-)-PHX. With respect to

Downloaded from dmd.aspetjournals.org at ASPET Journals on April 10, 2024

DMD Fast Forward. Published on October 18, 2006 as DOI: 10.1124/dmd.106.012252
This article has not been copyedited and formatted. The final version may differ from this version.

PM HLM, the Cl_{int} of (+)- and (-)-PHX by *trans1*- or *trans2*-4-monohydroxylation was similar.

CYP isoform-specific chemical inhibition studies

EM and IM HLM

Cis-OH-(+)- and *cis*-OH-(-)-PHX formation was significantly inhibited by quinidine (91 ± 6%, p=0.002 and 94 ± 6%, p=0.006, respectively) (Figure 5A).The high affinity formation of *trans1*-OH-(+)-PHX was significantly inhibited by troleandomycin (43 ± 2%, p=0.018) and quinidine (30 ± 22%, p=0.034). The low affinity formation of this metabolite was significantly inhibited by thio-TEPA (27 ± 9%, p=0.047), troleandomycin (57 ± 2%, p=0.013) and quinidine (16 ± 5%, p=0.005) and was significantly increased by coumarin (83 ± 35%, p=0.019). *Trans1*-OH-(-)-PHX formation was significantly inhibited by *S*-mephenytoin (16 ± 3%, p=0.039), thio-TEPA (41 ± 5%, p=0.021) and troleandomycin (74 ± 2%, p=0.020) and was significantly increased by coumarin (231 ± 50%, p=0.003) (Figure 5B). *Trans2*-OH-(+)-PHX formation was significantly inhibited by thio-TEPA (43 ± 6%, p=0.047) and troleandomycin (79 ± 8%, p=0.018) and was significantly increased by coumarin (190 ± 45%, p=0.011). *Trans2*-OH-(-)-PHX formation was significantly inhibited by thio-TEPA (29 ± 3%, p=0.025) and troleandomycin (68 ± 15%, p=0.019) and was significantly increased by coumarin (197 ± 54%, p=0.006) (Figure 5C).

PM HLM

Downloaded from dmd.aspetjournals.org at ASPET Journals on April 10, 2024

DMD Fast Forward. Published on October 18, 2006 as DOI: 10.1124/dmd.106.012252
This article has not been copyedited and formatted. The final version may differ from this version.

Trans1-OH-(+)-PHX formation was inhibited 36% by thio-TEPA and 77% by troleandomycin and was increased 171% by coumarin. *Trans1*-OH-(-)-PHX formation was inhibited 33% by thio-TEPA and 84% by troleandomycin and was increased 262% by coumarin (Figure 6A). *Trans2*-OH-(+)-PHX formation was inhibited 36% by thio-TEPA and 81% by troleandomycin and was increased 161% by coumarin. *Trans2*-OH-(-)-PHX formation was inhibited 29% by thio-TEPA and 77% by troleandomycin and was increased 224% by coumarin (Figure 6B).

Inhibition by CYP isoform-specific monoclonal antibodies

Cis-OH-(+)-PHX and *cis*-OH-(-)-PHX formation was inhibited 65% and 74%, respectively, by MAB-2D6 (Figure 7A). The high affinity formation of *trans1*-OH-(+)-PHX was inhibited 34% by MAB-3A4 and 34% by MAB-2D6. The low affinity formation of this metabolite was inhibited 21% by MAB-3A4, 19% by MAB-2D6 and 21% by MAB-2B6. *Trans1*-OH-(-)-PHX formation was inhibited 45% by MAB-3A4 and 27% by MAB-2B6 (Figure 7B). *Trans2*-OH-(+)-PHX formation was inhibited 41% by MAB-3A4 and 27% by MAB-2B6. *Trans2*-OH-(-)-PHX formation was inhibited 35% by MAB-3A4 and 32% by MAB-2B6 (Figure 7C).

Metabolism by recombinant expressed human CYP isoforms

Recombinant expressed CYP2B6 and CYP3A4 similarly catalysed the formation of *trans1*-OH-(+)-PHX, *trans1*-OH-(-)-PHX, *trans2*-OH-(+)-PHX and *trans2*-OH-(-)-PHX. Recombinant expressed CYP2D6 catalysed the formation of *cis*-OH-(+)-PHX, *cis*-OH-(-)-PHX and *trans1*-OH-(+)-PHX. Recombinant expressed CYP2C19 or the

Downloaded from dmd.aspetjournals.org at ASPET Journals on April 10, 2024

DMD Fast Forward. Published on October 18, 2006 as DOI: 10.1124/dmd.106.012252
This article has not been copyedited and formatted. The final version may differ from this version.

expression vectors without *CYP* cDNA did not metabolise (+)- or (-)-PHX to any of the 4-monohydroxy metabolites (data not shown).

Metabolism by recombinant expressed human CYP3A4 and 100μM coumarin

Trans1-OH-(+)-PHX, *trans1*-OH-(-)-PHX, *trans2*-OH-(+)-PHX and *trans2*-OH-(-)-PHX formation by recombinant expressed CYP3A4 was increased 108%, 120%, 119% and 124%, respectively, by coincubation with coumarin (data not shown).

Downloaded from dmd.aspetjournals.org at ASPET Journals on April 10, 2024

DMD Fast Forward. Published on October 18, 2006 as DOI: 10.1124/dmd.106.012252
This article has not been copyedited and formatted. The final version may differ from this version.

DISCUSSION

The microsomal data from this study unequivocally demonstrate that both enantiomers of PHX are subject to significant polymorphic metabolism by CYP2D6, although this enzyme exhibits distinct stereoselectivity with respect to the conformation of metabolites and the rate at which they are formed, consistent with the enantioselective pharmacokinetics observed *in vivo* for CYP2D6 EM (Gould et al., 1986, Inglis et al., in press). This study is the first to identify the involvement of CYP2B6 and CYP3A4 in the metabolism of PHX. They are minor contributors to the intrinsic CYP-mediated hepatic clearance of both enantiomers, except in CYP2D6 PM. Metabolism by these two enzymes does not display any distinct stereoselectivity and is therefore unable to explain the significant enantioselectivity observed *in vivo* for PM (Inglis et al., in press).

PHX is a weak lipophilic base and non-specific binding in microsomal incubations can markedly influence the choice of kinetic model describing metabolite formation and interpretation (McLure et al., 2000). Binding of each PHX enantiomer was saturable across the range of substrate concentrations employed and was described by a standard binding model, but did not exhibit any distinct enantioselectivity. Free substrate concentrations in microsomal incubations were calculated to prevent erroneous sigmoidal transformations of reaction curves (McLure et al., 2000). For most of the kinetic data, better fits were obtained by incorporating substrate inhibition (Tracy and Hummel, 2004) in the Michaelis-Menten model. Uncompetitive substrate inhibition may be explained by a two-site binding model where one site is favoured for oxidation but binding of substrate to the second site (at higher concentrations)

Downloaded from dmd.aspetjournals.org at ASPET Journals on April 10, 2024

DMD Fast Forward. Published on October 18, 2006 as DOI: 10.1124/dmd.106.012252
This article has not been copyedited and formatted. The final version may differ from this version.

produces a substrate-enzyme-substrate complex less capable of forming product than the enzyme-substrate complex (Hutzler and Tracy, 2002). The calculated K_s values were greater than their corresponding K_m values as the substrate preferentially bound to the productive site and were generally above the range of substrate concentrations used in the microsomal incubations, yet this model was employed where it provided a statistically better solution in order to prevent the erroneous kinetic parameter estimations that can occur if a standard Michaelis-Menten hyperbolic curve is forced through the data (Houston and Kenworthy, 2000).

Formation of *cis*-OH-(+)- and *cis*-OH-(-)-PHX was below the limit of quantification in PM incubations, consistent with CYP2D6-mediated catalysis. For EM and IM, high affinity single enzyme Michaelis-Menten models best described the kinetics of *cis*-4-monohydroxylation for each enantiomer of PHX, except for the formation of *cis*-OH-(+)-PHX by one IM (# 36). These K_m values are within the range of unbound (+)- and (-)-PHX concentrations observed in clinical plasma specimens (Inglis et al., in press), and are consistent with the saturability of *cis*-4-monohydroxy metabolite formation at therapeutic concentrations *in vivo* (Sallustio et al., 2002). Sørensen et al. (2003) also reported a high affinity 4-monohydroxylation reaction by EM *in vitro*, although the K_m values were larger because they reflected total rather than unbound microsomal PHX concentrations. The mean contribution of *cis*-4-monohydroxylation to mean total Cl_{int} for (+)-PHX was 43% in EM and 12% in IM, and for (-)-PHX it was 99% and 89%, respectively. The lower contribution of *cis*-4-monohydroxylation to total Cl_{int} in IM can be explained by the lower expression of CYP2D6 in livers with only one functional *CYP2D6* allele when compared with EM subjects with two functional *CYP2D6* alleles (Zanger et al., 2001), producing correspondingly smaller V_{max} values.

Downloaded from dmd.aspetjournals.org at ASPET Journals on April 10, 2024

DMD Fast Forward. Published on October 18, 2006 as DOI: 10.1124/dmd.106.012252
This article has not been copyedited and formatted. The final version may differ from this version.

IM# 36 was genotyped as having only one functional allele, *CYP2D6*2J*, that has been characterised as having impaired *in vivo* function by sparteine phenotyping in two individuals (Raimundo et al., 2004). The significantly larger K_m observed in the current study suggests that the enzyme is defective, possibly as a result of an as yet undetermined post-transcriptional modification attributable to the 2939G>A single nucleotide polymorphism unique to the allele (Marez et al., 1997) producing a different protein to CYP2D6.2.

The *cis*-4-monohydroxylation of both enantiomers of PHX was effectively abolished by the CYP2D6 specific chemical inhibitor quinidine in EM and IM incubations, in agreement with Sørensen et al. (2003), and was inhibited by monoclonal antibodies directed against CYP2D6. Recombinant expressed CYP2D6 *cis*-4-monohydroxylated (+)- and (-)-PHX. When these findings are considered with the observation that this metabolite is effectively absent in PM, it can be concluded that the *cis*-4-monohydroxylation of both PHX enantiomers is catalysed exclusively by CYP2D6 (Figure 8). The mean Cl_{int} of (-)-PHX by *cis*-4-monohydroxylation was approximately 4- and 16-fold higher in EM and IM, respectively, than for (+)-PHX and is consistent with the enantioselective metabolism of (-)-PHX to *cis*-OH-(-)-PHX reported *in vivo* (Gould et al., 1986).

The formation of *trans1*-OH-(+)-PHX by the EM and by one IM (# 18) was catalysed by a high and a low affinity reaction. For the other IM (# 36) and both PM, only a single low affinity reaction was indicated. This suggested that CYP2D6 was the high affinity enzyme and was confirmed by the inhibition produced by quinidine and

Downloaded from dmd.aspetjournals.org at ASPET Journals on April 10, 2024

DMD Fast Forward. Published on October 18, 2006 as DOI: 10.1124/dmd.106.012252
This article has not been copyedited and formatted. The final version may differ from this version.

MAB-2D6 (Figure 8). With a similar affinity to *cis*-4-monohydroxylation, formation of *trans1*-OH-(+)-PHX by CYP2D6 is also likely to be a saturable process *in vivo*. The high affinity formation of *trans1*-OH-(+)-PHX was also inhibited by troleandomycin, indicating the involvement of CYP3A4, although the inhibition was greater with respect to the low affinity process. Involvement of CYP2B6 in the low affinity process was indicated by the inhibition produced by thio-TEPA. The roles of CYP3A4 and CYP2B6 in the low affinity formation of *trans1*-OH-(+)-PHX (Figure 8) were confirmed by the results of the chemical inhibitors in the PM and by the incubation of monoclonal antibodies with an EM (# 31). Incubations of recombinant expressed CYP2B6, CYP2D6 and CYP3A4 all produced *trans1*-OH-(+)-PHX. *Trans1*-OH-(+)-PHX formation was an important contributor to the mean total Cl_{int} of (+)-PHX, accounting for 56% in EM, 77% in IM and 48% in PM. For EM and IM, the mean Cl_{int} of (+)-PHX by *trans1*-4-monohydroxylation was approximately 33- and 5-fold higher, respectively, than for (-)-PHX and is consistent with observations *in vivo* (Gould et al., 1986).

The formation of *trans1*-OH-(-)-PHX was catalysed by a low affinity process in all HLM and as indicated by the inhibition studies was most likely mediated by CYP2B6 and CYP3A4 (Figure 8). This was confirmed by incubations of the recombinant expressed enzymes with (-)-PHX. Although the selective CYP2C19 inhibitor *S*-mephenytoin produced a small but statistically significant inhibition of *trans1*-OH-(-)-PHX formation, the role of CYP2C19 was subsequently excluded from involvement in this metabolic pathway because incubations of (-)-PHX with the recombinant expressed human CYP2C19 enzyme did not produce any detectable metabolite. *Trans1*-OH-(-)-PHX formation was a minor contributor to the mean total Cl_{int} of (-)-

Downloaded from dmd.aspetjournals.org at ASPET Journals on April 10, 2024

DMD Fast Forward. Published on October 18, 2006 as DOI: 10.1124/dmd.106.012252
This article has not been copyedited and formatted. The final version may differ from this version.

PHX in EM and IM, accounting for only 1 and 7%, respectively, due to the very high clearance of (-)-PHX by CYP2D6-mediated *cis*-4-monohydroxylation. In contrast, formation of *trans1*-OH-(-)-PHX was responsible for 64% of the mean total Cl_{int} of (-)-PHX in PM.

The kinetics and CYP isoform profile of the formation of *trans2*-OH-(+)- and *trans2*-OH-(-)-PHX was similar to that of *trans1*-OH-(-)-PHX. A single low affinity reaction was indicated for all HLM and inhibition studies determined that their formation was mediated by CYP2B6 and CYP3A4. This was confirmed by incubations of recombinant expressed CYP2B6 and CYP3A4 with each PHX enantiomer. The formation of the *trans2*-4-monohydroxy metabolites from both enantiomers was similar in all HLM, and was only a significant contributor to mean total Cl_{int} in PM due to the larger contributions of CYP2D6-mediated 4-monohydroxylation in EM and IM. With respect to the mean total Cl_{int} of (+)-PHX, *trans2*-OH-(+)-PHX formation accounted for 2% in EM, 11% in IM and 52% in PM. For (-)-PHX, *trans2*-OH-(-)-PHX formation accounted for <1% in EM, 4% in IM and 36% in PM.

The data clearly demonstrate that CYP2D6 is the major enzyme catalysing the metabolism of both (+)- and (-)-PHX by EM and IM, in agreement with the *in vivo* findings of Inglis et al. (in press). Formation of *cis*-OH-(-)-PHX by CYP2D6 accounts for 99% and 89% of the mean total Cl_{int} of (-)-PHX by EM and IM, respectively, and formation of *trans1*-OH-(+)-PHX and *cis*-OH-(+)-PHX by CYP2D6 accounts for 97% and 76% of the mean total Cl_{int} of (+)-PHX by EM and IM, respectively. Interestingly, whilst CYP2D6-catalysed *cis*-4-monohydroxylation was enantioselective for (-)-PHX, CYP2D6-catalysed *trans1*-4-monohydroxylation was

Downloaded from dmd.aspetjournals.org at ASPET Journals on April 10, 2024

DMD Fast Forward. Published on October 18, 2006 as DOI: 10.1124/dmd.106.012252
This article has not been copyedited and formatted. The final version may differ from this version.

enantiospecific for (+)-PHX. The importance of CYP3A4 and CYP2B6 in PHX metabolism increases as the contribution of CYP2D6 decreases, such that these two enzymes account for the majority of hepatic P450 mediated clearance in PM (Figure 8), with the inhibitor studies suggesting a proportionately larger role for CYP3A4 than CYP2B6. Neither of these P450 isoforms exhibits any clear enantioselectivity for PHX metabolism, as indicated by the kinetics in PM. The distinct enantioselectivity of PHX metabolism displayed by PM *in vivo* (Inglis et al., in press) may be due to extra-hepatic metabolism, non-CYP metabolism or transporters involved in absorption, renal, biliary or intestinal excretion, and merits further investigation.

CYP3A is the most abundant P450 in the liver (Shimada et al., 1994) and is composed primarily of CYP3A4, except in approximately one quarter of Caucasians, carrying at least one *CYP3A5*1* allele, where CYP3A5 constitutes at least half of total hepatic CYP3A (Lin et al., 2002). CYP3A5 may be involved in PHX metabolism because CYP3A4 and CYP3A5 have similar substrate specificity (Gillam et al., 1995) and the 3-fold range in the oral clearance of five PM observed by Sallustio et al. (2002) may be due to interindividual differences in CYP3A expression (Lin et al., 2002). CYP2B6 shares regulatory features with CYP3A4 (Rodriguez-Antona et al., 2000) and its expression is also highly variable (Stresser and Kupfer, 1999). It constitutes approximately 6% of total hepatic P450 (Stresser and Kupfer, 1999) and its importance in drug metabolism is increasing as more substrates are recognised (Bertz and Granneman, 1997, Ekins and Wrighton, 1999, Lewis et al., 2002, Rendic, 2002), although the functional consequences of polymorphisms of *CYP2B6* have not yet been fully elucidated (Daly, 2004).

Downloaded from dmd.aspetjournals.org at ASPET Journals on April 10, 2024

DMD Fast Forward. Published on October 18, 2006 as DOI: 10.1124/dmd.106.012252
This article has not been copyedited and formatted. The final version may differ from this version.

The CYP2A6 specific inhibitor coumarin enhanced the *trans1*- and *trans2*-hydroxylation of both enantiomers of PHX in all HLM. This effect was not observed for the CYP2D6-dependent formation of *cis*-OH-(+)- or *cis*-OH-(-)-PHX. Heterotropic cooperativity by CYP3A4 has been reported in the literature for several substrates in various *in vitro* systems (Hutzler and Tracy, 2002), but not for CYP2B6. Because coumarin is a substrate of CYP3A4 (Born et al., 2002), the possibility that it is a positive effector of (+)- and (-)-PHX metabolism by CYP3A4 was investigated by coincubating coumarin, (+)- or (-)-PHX and recombinant expressed human CYP3A4. *Trans1*- and *trans2*-4-monohydroxylation of both enantiomers was increased over 100%. The heterotropic cooperativity of CYP3A4 has been observed mainly *in vitro*. Corresponding *in vivo* data are rare (Tang and Stearns, 2001). Further studies need to be undertaken to determine whether enhanced metabolism of PHX occurs *in vivo* in order to assess its potential to cause drug-drug interactions, particularly in PM, for whom CYP3A4-mediated metabolism is a primary determinant of PHX clearance. Importantly, the data demonstrate that the use of coumarin as a specific inhibitor of CYP2A6 may be confounded by possible heterotropic cooperative interactions with other compounds that are also CYP3A4 substrates.

In conclusion, CYP2D6 is the major enzyme catalysing the 4-monohydroxylation of both (+)- and (-)-PHX in EM and IM. It displays K_m values within the range of unbound concentrations in plasma attained clinically for both enantiomers of PHX. Thus, saturable and polymorphic CYP2D6 metabolism underlies the extreme variability in the pharmacokinetics of both PHX enantiomers *in vivo*. CYP3A4 and CYP2B6 are the major enzymes responsible for the 4-monohydroxylation of (+)- and (-)-PHX in PM, and did not show appreciable enantioselectivity. This is in contrast to

Downloaded from dmd.aspetjournals.org at ASPET Journals on April 10, 2024

DMD Fast Forward. Published on October 18, 2006 as DOI: 10.1124/dmd.106.012252
This article has not been copyedited and formatted. The final version may differ from this version.

the significant enantioselectivity in the pharmacokinetics of (+)- and (-)-PHX observed clinically in PM.

Downloaded from dmd.aspetjournals.org at ASPET Journals on April 10, 2024

DMD Fast Forward. Published on October 18, 2006 as DOI: 10.1124/dmd.106.012252
This article has not been copyedited and formatted. The final version may differ from this version.

ACKNOWLEDGMENTS

We thank Dr Elizabeth Gillam for supplying recombinant expressed human CYP2B6.

Downloaded from dmd.aspetjournals.org at ASPET Journals on April 10, 2024

DMD Fast Forward. Published on October 18, 2006 as DOI: 10.1124/dmd.106.012252
This article has not been copyedited and formatted. The final version may differ from this version.

REFERENCES

Baldwin S, Bloomer J, Smith G, Ayrton A, Clarke S and Chenery R (1995) Ketoconazole and sulphaphenazole as the respective selective inhibitors of P4503A and 2C9. *Xenobiotica* **25**: 261-270.

Bertz RJ and Granneman GR (1997) Use of in vitro and in vivo data to estimate the likelihood of metabolic pharmacokinetic interactions. *Clin Pharmacokinet* **32**: 210-258.

Born SL, Caudill D, Fliter KL and Purdon MP (2002) Identification of the cytochromes P450 that catalyze coumarin 3,4-epoxidation and 3-hydroxylation. *Drug Metab Dispos* **30**: 483-487.

Cole PL, Beamer AD, McGowan N, Cantillon CO, Benfell K, Kelly RA, Hartley LH, Smith TW and Antman E (1990) Efficacy and safety of perhexiline maleate in refractory angina. A double-blind placebo-controlled clinical trial of a novel antianginal agent. *Circulation* **81**: 1260-1270.

Cooper JDH, Turnell DC, Pilcher J and Lockhart D (1985) Therapeutic monitoring of the anti-anginal drug perhexiline maleate. *Ann Clin Biochem* **22**: 614-617.

Cooper RG, Evans DAP and Whibley EJ (1984) Polymorphic hydroxylation of perhexiline maleate in man. *J Med Genetics* **21**: 27-33.

Downloaded from dmd.aspetjournals.org at ASPET Journals on April 10, 2024

DMD Fast Forward. Published on October 18, 2006 as DOI: 10.1124/dmd.106.012252
This article has not been copyedited and formatted. The final version may differ from this version.

Daly AK (2004) Pharmacogenetics of the cytochromes P450. *Curr Top Med Chem* **4**: 1733-1744.

Davies BJ, Herbert MK, Culbert JA, Pyke SM, Coller JK, Somogyi AA, Milne RW and Sallustio BC (2006a) Enantioselective assay for the determination of perhexiline enantiomers in human plasma by liquid chromatography. *J Chromatogr B* **832**: 114-120.

Davies BJ, Herbert MK, Coller JK, Somogyi AA, Milne RW and Sallustio BC (in press) Determination of the 4-monohydroxy metabolites of perhexiline in human plasma, urine and liver microsomes by liquid chromatography. *J Chromatogr B.*

Davies BJ, Coller JK, James HM, Somogyi AA, Horowitz JD and Sallustio BC (2006b) The influence of CYP2D6 genotype on trough plasma perhexiline and *cis*-OH-perhexiline concentrations following a standard loading regimen in patients with myocardial ischaemia. *Br J Clin Pharmacol* **61**: 321-325.

Ekins S and Wrighton SA (1999) The role of CYP2B6 in human xenobiotic metabolism. *Drug Metab Rev* **31**: 719-754.

Gillam EM, Guo Z, Ueng YF, Yamazaki H, Cock I, Reilly PE, Hooper WD and Guengerich FP (1995) Expression of cytochrome P450 3A5 in Escherichia coli: effects of 5' modification, purification, spectral characterization, reconstitution conditions, and catalytic activities. *Arch Biochem Biophys* **317**: 374-384.

Downloaded from dmd.aspetjournals.org at ASPET Journals on April 10, 2024

DMD Fast Forward. Published on October 18, 2006 as DOI: 10.1124/dmd.106.012252
This article has not been copyedited and formatted. The final version may differ from this version.

Gould BJ, Amoah AGB and Parke DV (1986) Stereoselective pharmacokinetics of perhexiline. *Xenobiotica* **16**: 491-502.

Houston JB and Kenworthy KE (2000) In vitro-in vivo scaling of CYP kinetic data not consistent with the classical Michaelis-Menten model. *Drug Metab Dispos* **28**: 246-254.

Hutchinson MR, Menelaou A, Foster DJR, Coller JK and Somogyi AA (2004) CYP2D6 and CYP3A4 involvement in the primary oxidative metabolism of hydrocodone by human liver microsomes. *Br J Clin Pharmacol* **57**: 287-297.

Hutzler JM and Tracy TS (2002) Atypical kinetic profiles in drug metabolism reactions. *Drug Metab Dispos* **30**: 355-362.

Inglis SC, Herbert MK, Davies BJ, Coller JK, James HM, Horowitz JD, Morris RG, Milne RW, Somogyi AA and Sallustio BC (in press) Effect of CYP2D6 metaboliser status on the disposition of the (+)- and (-)-enantiomers of perhexiline in patients with myocardial ischaemia. *Pharmacogenet Genomics*.

James HM, Coller JK, Gillis D, Bahnisch J, Sallustio BC and Somogyi AA (2004) A new simple diagnostic assay for the identification of the major *CYP2D6* genotypes by DNA sequencing analysis. *Int J Clin Pharmacol Ther* **42**: 719-723.

Lewis DF, Modi S and Dickins M (2002) Structure-activity relationship for human cytochrome P450 substrates and inhibitors. *Drug Metab Rev* **34**: 69-82.

Downloaded from dmd.aspetjournals.org at ASPET Journals on April 10, 2024

DMD Fast Forward. Published on October 18, 2006 as DOI: 10.1124/dmd.106.012252
This article has not been copyedited and formatted. The final version may differ from this version.

Lin YS, Dowling AL, Quigley SD, Farin FM, Zhang J, Lamba J, Schuetz EG and Thummel KE (2002) Co-regulation of CYP3A4 and CYP3A5 and contribution to hepatic and intestinal midazolam metabolism. *Mol Pharmacol* **62**: 162-172.

Lowry OH, Roseburg NJ, Farr AL and Randall RJ (1951) Measurement with the Folin phenol reagent. *J Biol Chem* **193**: 265-275.

Marez D, Legrand M, Sabbagh N, Guidice JM, Spire C, Lafitte JJ, Meyer UA and Broly F (1997) Polymorphism of the cytochrome P450 CYP2D6 gene in a European population: characterization of 48 mutations and 53 alleles, their frequencies and evolution. *Pharmacogenetics* **7**: 193-202.

McLure JA, Miners JO and Birkett DJ (2000) Nonspecific binding of drugs to human liver microsomes. *Br J Clin Pharmacol* **49**: 453-461.

Morgan MY, Reshef R, Shah RR, Oates NS, Smith RL and Sherlock S (1984) Impaired oxidation of debrisoquine in patients with perhexiline liver injury. *Gut* **25**: 1057-1064.

Newton D, Wang R and Lu A (1995) Cytochrome P450 inhibitors: Evaluation of specificities in the in vitro metabolism of therapeutic agents by human liver microsomes. *Drug Metab Dispos* **23**: 154-158.

Downloaded from dmd.aspetjournals.org at ASPET Journals on April 10, 2024

DMD Fast Forward. Published on October 18, 2006 as DOI: 10.1124/dmd.106.012252
This article has not been copyedited and formatted. The final version may differ from this version.

Notley LM, de Wolf CJ, Wunsch RM, Lancaster RG and Gillam EM (2002) Bioactivation of tamoxifen by recombinant human cytochrome P450 enzymes. *Chem Res Toxicol* **15**: 614-622.

Omura T and Sato R (1964) The carbon monoxide-binding pigment of liver microsomes, II. Solubilisation, purification and properties. *J Biol Chem* **234**; 2374-2385.

Rae JM, Soukhova NV, Flockhart DA and Desta Z (2002) Triethylenephosphoramide is a specific inhibitor of cytochrome P450 2B6: implications for cyclophosphoramide metabolism. *Drug Metab Dispos* **30**: 525-530.

Raimundo S, Toscano C, Klein K, Fischer J, Griese EU, Eichelbaum M, Schwab M and Zanger UM (2004) A novel intronic mutation, 2988G>A, with high predictivity for impaired function of cytochrome P450 2D6 in white subjects. *Clin Pharmacol Ther* **76**: 128-138.

Rendic S (2002) Summary of information on human CYP enzymes: human P450 metabolism data. *Drug Metab Rev* **34**: 83-448.

Rodriguez-Antona C, Jover R, Gomez-Lechon MJ and Castell JV (2000) Quantitative RT-PCR measurement of human cytochrome P-450s: application to drug induction studies. *Arch Biochem Biophys* **376**: 109-116.

Downloaded from dmd.aspetjournals.org at ASPET Journals on April 10, 2024

DMD Fast Forward. Published on October 18, 2006 as DOI: 10.1124/dmd.106.012252
This article has not been copyedited and formatted. The final version may differ from this version.

Sallustio BC, Westley IC and Morris RG (2002) Pharmacokinetics of the antianginal agent perhexiline: relationship between metabolic ratio and steady state dose. *Br J Clin Pharmacol* **54**: 107-114.

Shah RR, Oates NS, Idle JR, Smith RL and Lockhart JDF (1982) Impaired oxidation of debrisoquine in patients with perhexiline neuropathy. *Br Med J* **284**: 295-299.

Shimada T, Yamazaki H, Mimura M, Inui Y and Guengerich FP (1994) Interindividual variations in human liver cytochrome P-450 enzymes involved in the oxidation of drugs, carcinogens and toxic chemicals: studies with liver microsomes of 30 Japanese and 30 Caucasians. *J Pharmacol Exp Ther* **270**: 414-423.

Sørensen LB, Sørensen RN, Miners JO, Somogyi AA, Grgurinovich N and Birkett DJ (2003) Polymorphic hydroxylation of perhexiline *in vitro*. *Br J Clin Pharmacol* **55**: 635-638.

Stresser DM and Kupfer D (1999) Monospecific antipeptide antibody to cytochrome P-450 2B6. *Drug Metab Dispos* **27**: 517-525.

Tang W and Stearns RA (2001) Heterotropic cooperativity of cytochrome P450 3A4 and potential drug-drug interactions. *Curr Drug Metab* **2**: 185-198.

Tracy TS and Hummel MA (2004) Modeling kinetic data from in vitro drug metabolism enzyme experiments. *Drug Metab Rev* **36**: 231-242.

Downloaded from dmd.aspetjournals.org at ASPET Journals on April 10, 2024

DMD Fast Forward. Published on October 18, 2006 as DOI: 10.1124/dmd.106.012252
This article has not been copyedited and formatted. The final version may differ from this version.

Tucker GT, Houston JB and Huang SM (2001) Optimizing drug development: strategies to assess drug metabolism/transporter interaction potential – towards a consensus. *Br J Clin Pharmacol* **52**: 107-117.

Zanger UM, Fischer J, Raimundo S, Stuven T, Evert BO, Schwab M and Eichelbaum M (2001) Comprehensive analysis of the genetic factors determining expression and function of hepatic CYP2D6. *Pharmacogenetics* **11**: 573-585.

Zanger UM, Vilbois F, Hardwick JP and Meyer UA (1988) Absence of hepatic cytochrome P450bufI causes genetically deficient debrisoquine oxidation in man. *Biochemistry* **27**: 5447-5454.

Downloaded from dmd.aspetjournals.org at ASPET Journals on April 10, 2024

DMD Fast Forward. Published on October 18, 2006 as DOI: 10.1124/dmd.106.012252
This article has not been copyedited and formatted. The final version may differ from this version.

FOOTNOTES

This work was funded by a project grant from the National Heart Foundation of Australia. BJL Davies is the recipient of the MF and MH Joyner Scholarship in Medicine and the Freemasons Medical Research Scholarship of the Faculty of Health Sciences, University of Adelaide.

This work was presented in part at the 2005 Scientific Meeting of the Australasian Society of Clinical and Experimental Pharmacologists and Toxicologists.
Davies BJL, Sallustio BC, Somogyi AA, Coller JK and Milne RW (2005) *In vitro* enantioselective human metabolism of perhexiline. *Proc Aust Soc Clin Exp Pharmacol Toxicol* **11**: 162.

Reprint requests
Benedetta C Sallustio
Department of Cardiology and Clinical Pharmacology, The Queen Elizabeth Hospital, 28 Woodville Road, Woodville, SA 5011, Australia
Telephone +61 8 8222 6510
Fax +61 8 8222 6033
E-mail benedetta.sallustio@nwahs.sa.gov.au

Downloaded from dmd.aspetjournals.org at ASPET Journals on April 10, 2024

DMD Fast Forward. Published on October 18, 2006 as DOI: 10.1124/dmd.106.012252
This article has not been copyedited and formatted. The final version may differ from this version.

LEGENDS FOR FIGURES

Figure 1. The chemical structures of the 4-monohydroxy metabolites of perhexiline. Chiral centres are indicated with an asterisk.

Figure 2. Binding of (+)-PHX (squares, solid line) and (-)-PHX (triangles, dashed line) to human liver microsomes (protein concentration 0.25 mg/ml).

Figure 3. Kinetic profile of *cis*-OH-(+)-PHX and *cis*-OH-(-)-PHX formation (A and B, respectively), *trans1*-OH-(+)-PHX and *trans1*-OH-(-)-PHX formation (C and D, respectively) and *trans2*-OH-(+)-PHX and *trans2*-OH-(-)-PHX formation (E and F, respectively) in human liver microsomes from a *CYP2D6* EM (# 46), a *CYP2D6* IM (# 36) and a *CYP2D6* PM (# 39).

Figure 4. Intrinsic clearance of (+)- and (-)-PHX by the three 4-monohydroxylation metabolic pathways (*cis*-hydroxylation black columns, *trans1*- hydroxylation white columns, *trans2*- hydroxylation hatched columns) by *CYP2D6* EM (n=3), IM (n=2) and PM (n=2) human liver microsomes.

Figure 5. Chemical inhibition of *cis*-4-monohydroxylation (A), *trans1*-4-monohydroxylation (B) and *trans2*-4-monohydroxylation (C) of (-)-PHX (white columns) and (+)-PHX (high affinity site - black columns, low affinity site – grey columns) by human liver microsomes from three *CYP2D6* EM and one *CYP2D6* IM. Data are the mean of triplicate determinations. Error bars indicate SD.

Downloaded from dmd.aspetjournals.org at ASPET Journals on April 10, 2024

DMD Fast Forward. Published on October 18, 2006 as DOI: 10.1124/dmd.106.012252
This article has not been copyedited and formatted. The final version may differ from this version.

Figure 6. Chemical inhibition of *trans1*-4-monohydroxylation (A) and *trans2*-4-monohydroxylation (B) of (-)-PHX (white columns) and (+)-PHX (black columns) by human liver microsomes from one *CYP2D6* PM. Data are the mean of triplicate determinations.

Figure 7. Inhibition of *cis*-4-monohydroxylation (A), *trans1*-4-monohydroxylation (B) and *trans2*-4-monohydroxylation (C) of (-)-PHX (white columns) and (+)-PHX (high affinity site - black columns, low affinity site – grey columns) by monoclonal antibodies directed towards human CYPs in human liver microsomes from a *CYP2D6* EM. Data are the mean of duplicate determinations.

Figure 8. Formation of the 4-monohydroxy metabolites of (+)-PHX (A) and (-)-PHX (B) and the CYP isoforms responsible.

Downloaded from dmd.aspetjournals.org at ASPET Journals on April 10, 2024

DMD Fast Forward. Published on October 18, 2006 as DOI: 10.1124/dmd.106.012252
This article has not been copyedited and formatted. The final version may differ from this version.

Table 1. Kinetic parameters for the *cis*- (A), *trans1*- (B) and *trans2*-4-monohydroxylation (C) of (+)- and (-)-perhexiline by human liver microsomes from three *CYP2D6* extensive metabolisers (EM), two *CYP2D6* intermediate metabolisers (IM) and two *CYP2D6* poor metabolisers (PM). V_{max} is the maximum rate of formation, K_m is the Michaelis-Menten constant, Cl_{int} is the intrinsic clearance calculated as V_{max} / K_m and K_s is the substrate inhibitor constant.

Downloaded from dmd.aspetjournals.org at ASPET Journals on April 10, 2024

Table 1A.

	CYP2D6 EM HLM				*CYP2D6* IM HLM			*CYP2D6* PM HLM		
	#21	#31	#46	Mean ± SD	#18	#36	Mean ± SD	#24	#39	Mean ± SD
Cis-OH-(+)-PHX										
V_{max} (pmol/min/mg)	15.9	12.2	18.8	15.6 ± 3.3	8.0	9.8	8.9 ± 1.2	-	-	-
K_m (μM)	0.024	0.031	0.026	0.027 ± 0.003	0.16	2.5	1.4 ± 1.7	-	-	-
K_s (μM)	-	-	257	257	-	258	258	-	-	-
Cl_{int} (μl/min/mg)	650	397	712	586 ± 167	50.2	3.8	27.0 ± 32.8	-	-	-
Cis-OH-(-)-PHX										
V_{max} (pmol/min/mg)	98.3	81.4	141.9	107.2 ± 31.2	35.9	11.7	23.8 ± 17.1	-	-	-
K_m (μM)	0.047	0.032	0.052	0.044 ± 0.011	0.048	0.104	0.076 ± 0.040	-	-	-
K_s (μM)	104.9	180.5	117.4	134.3 ± 40.5	346.6	-	346.6	-	-	-
Cl_{int} (μl/min/mg)	2078	2534	2708	2439 ± 326	747	113	430 ± 449	-	-	-

Downloaded from dmd.aspetjournals.org at ASPET Journals on April 10, 2024

DMD Fast Forward. Published on October 18, 2006 as DOI: 10.1124/dmd.106.012252
This article has not been copyedited and formatted. The final version may differ from this version.

Table 1B.

	CYP2D6 EM HLM				*CYP2D6* IM HLM			*CYP2D6* PM HLM		
	#21	#31	#46	Mean ± SD	#18	#36	Mean ± SD	#24	#39	Mean ± SD
Trans1-OH-(+)-PHX (high affinity)										
V_{max} (pmol/min/mg)	16.7	10.1	21.1	16.0 ± 5.5	4.5	-	4.5	-	-	-
K_m (μM)	0.023	0.017	0.023	0.021 ± 0.003	0.015	-	0.015	-	-	-
K_s (μM)	12.2	1.9	8.6	7.6 ± 5.2	-	-	-	-	-	-
Cl_{int} (μl/min/mg)	729	584	922	745 ± 169	298	-	298	-	-	-
Trans1-OH-(+)-PHX (low affinity)										
V_{max} (pmol/min/mg)	61.7	42.0	34.5	46.1 ± 14.1	43.7	94.4	69.1 ± 35.9	59.8	68.0	63.9 ± 5.8
K_m (μM)	2.1	1.8	1.6	1.9 ± 0.3	1.9	2.7	2.3 ± 0.6	1.9	2.2	2.1 ± 0.2
K_s (μM)	78.8	92.1	413	195 ± 189	-	185	185	68.7	29.2	49.0 ± 27.9
Cl_{int} (μl/min/mg)	29.5	22.8	21.5	24.6 ± 4.3	22.5	34.6	28.5 ± 8.5	30.9	30.4	30.6 ± 0.3
Trans1-OH-(-)-PHX										

Downloaded from dmd.aspetjournals.org at ASPET Journals on April 10, 2024

DMD Fast Forward. Published on October 18, 2006 as DOI: 10.1124/dmd.106.012252
This article has not been copyedited and formatted. The final version may differ from this version.

V_{max} (pmol/min/mg)	64.3	46.1	38.1	49.5 ± 13.5	47.8	125.5	86.7 ± 54.8	98.1	66.2	82.1 ± 22.5
K_m (μM)	2.4	2.2	1.8	2.1 ± 0.3	1.8	3.3	2.6 ± 1.1	2.9	1.9	2.4 ± 0.7
K_s (μM)	37.7	49.4	95.3	60.8 ± 30.5	256	115	186 ± 100	17.5	53.8	35.7 ± 25.6
Cl_{int} (μl/min/mg)	27.1	21.4	21.2	23.3 ± 3.3	27.2	37.5	32.4 ± 7.3	34.2	35.8	35.0 ± 1.1

DMD Fast Forward. Published on October 18, 2006 as DOI: 10.1124/dmd.106.012252
This article has not been copyedited and formatted. The final version may differ from this version.

Downloaded from dmd.aspetjournals.org at ASPET Journals on April 10, 2024

Table 1C.

	CYP2D6 EM HLM				*CYP2D6* IM HLM			*CYP2D6* PM HLM		
	#21	#31	#46	Mean ± SD	#18	#36	Mean ± SD	#24	#39	Mean ± SD
Trans2-OH-(+)-PHX										
V_{max} (pmol/min/mg)	50.4	26.1	23.5	33.3 ± 14.8	42.3	83.8	63.0 ± 29.3	53.9	71.9	62.9 ± 12.7
K_m (μM)	1.8	1.5	1.4	1.6 ± 0.2	2.2	2.6	2.4 ± 0.25	1.6	2.3	1.9 ± 0.5
K_s (μM)	45.2	73.5	67.4	62.0 ± 14.9	172	127	149 ± 32	60.0	23.5	41.8 ± 25.9
Cl_{int} (μl/min/mg)	28.8	17.0	16.3	20.7 ± 7.0	19.1	32.6	25.9 ± 9.6	33.6	31.9	32.7 ± 1.3
Trans2-OH-(-)-PHX										
V_{max} (pmol/min/mg)	38.4	29.5	26.7	31.5 ± 6.1	29.7	80.7	55.2 ± 36.0	61.3	37.7	49.5 ± 16.7
K_m (μM)	2.7	2.6	2.5	2.6 ± 0.1	1.8	3.7	2.8 ± 1.3	3.2	1.9	2.5 ± 0.9
K_s (μM)	46.2	57.3	104.8	69.4 ± 31.1	-	140	140	22.0	73.1	47.5 ± 36.1
Cl_{int} (μl/min/mg)	14.1	11.3	10.7	12.0 ± 1.8	16.2	21.9	19.1 ± 4.0	19.5	19.7	19.6 ± 0.1

Downloaded from dmd.aspetjournals.org at ASPET Journals on April 10, 2024

DMD Fast Forward. Published on October 18, 2006 as DOI: 10.1124/dmd.106.012252
This article has not been copyedited and formatted. The final version may differ from this version.

figure1

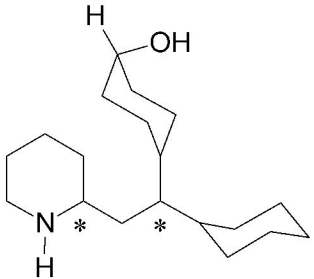

cis-OH-(+)-PHX

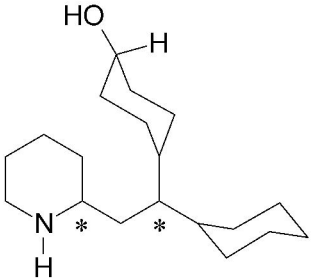

trans1-OH-(+)-PHX

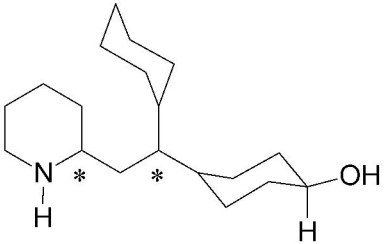

trans2-OH-(+)-PHX

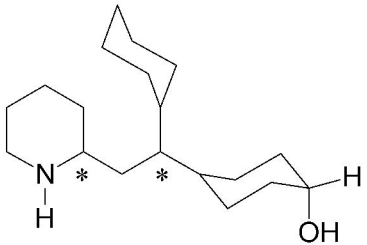

cis-OH-(-)-PHX

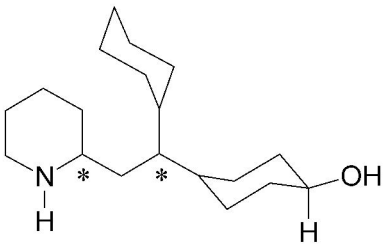

trans1-OH-(-)-PHX

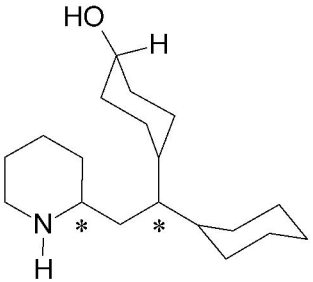

trans2-OH-(-)-PHX

figure 2

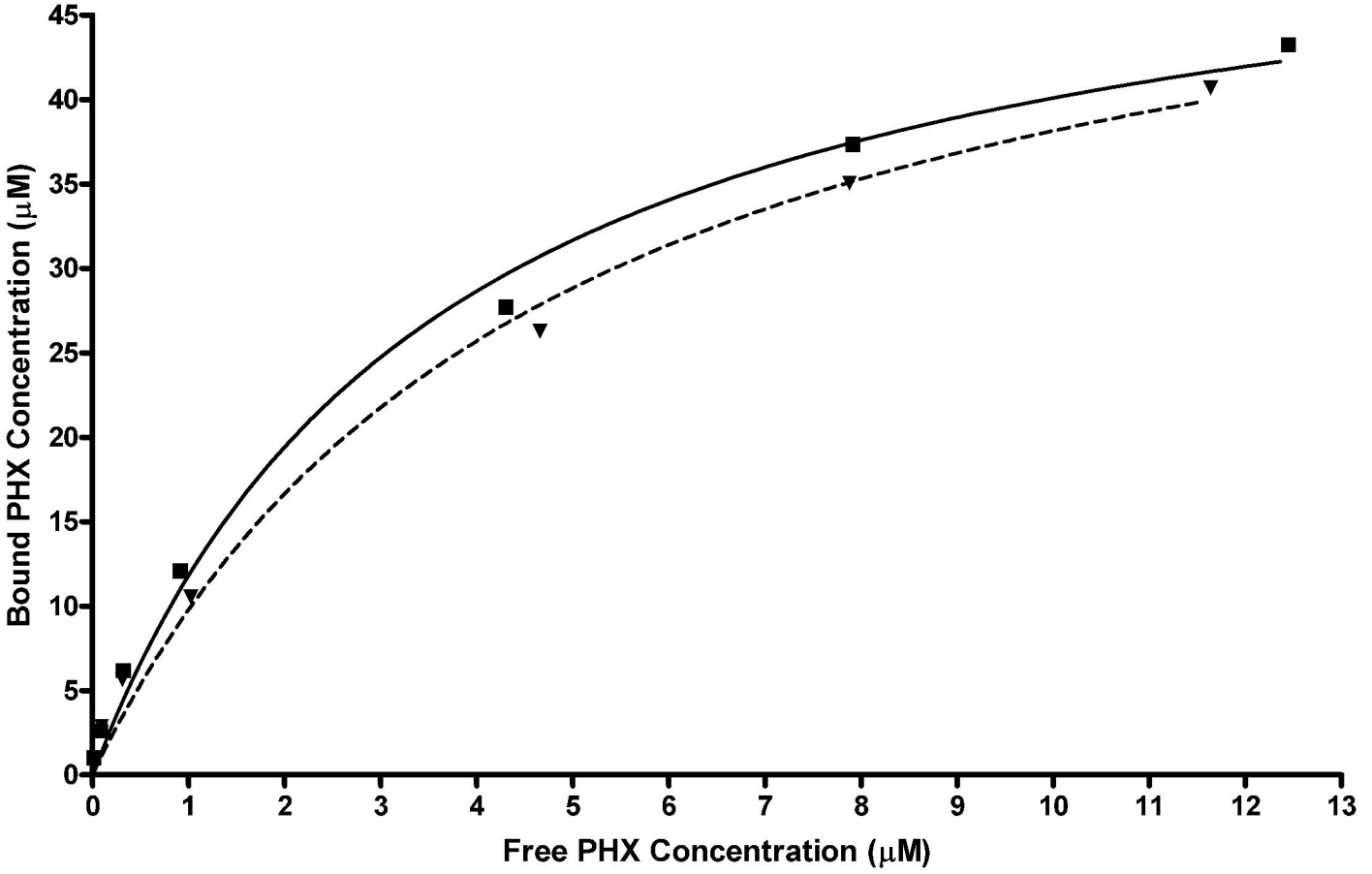
Bound PHX Concentration (μM)
45
40
35
30
25
20
15
10
5
0
0
1
2
3
4
5
6
7
8
9
10
11
12
13
Free PHX Concentration (μM)

figure 3a

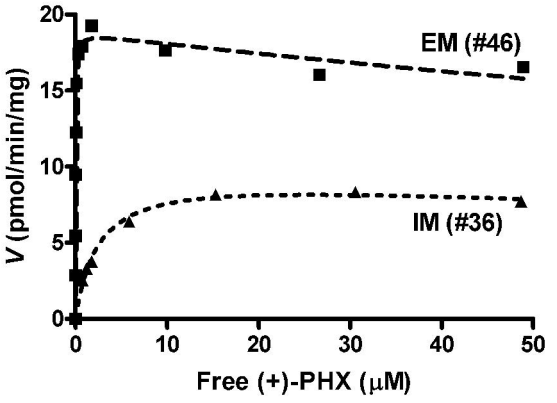

figure 3b

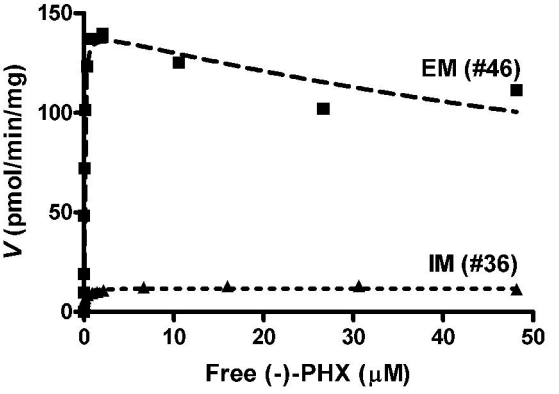

figure 3c

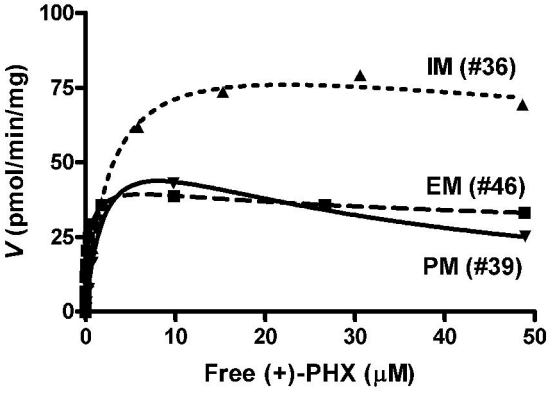

figure 3d

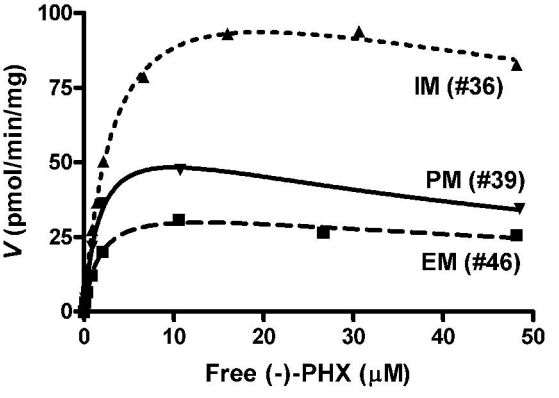

figure 3e

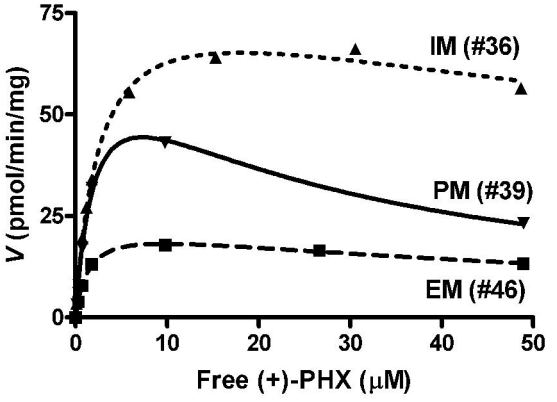

figure 3f

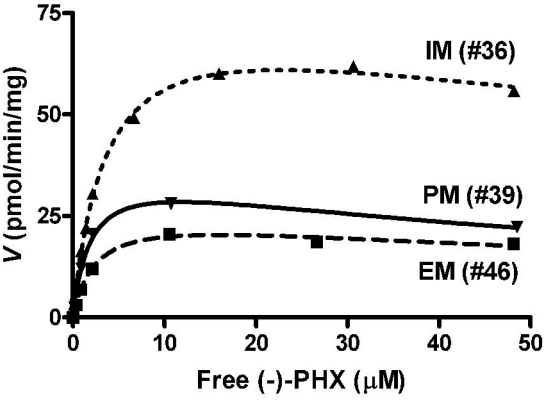

figure 4

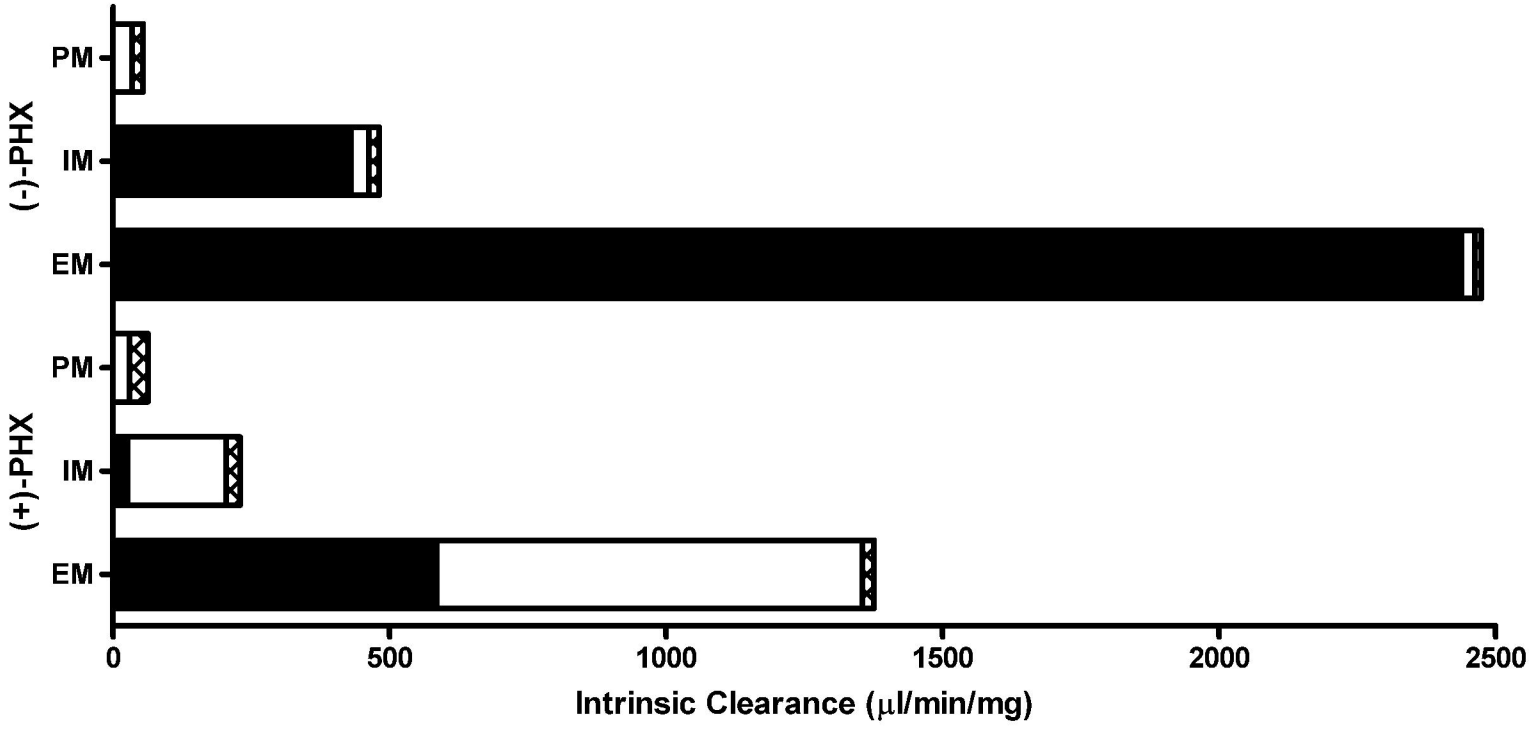

on April 10, 2024

figure 5a

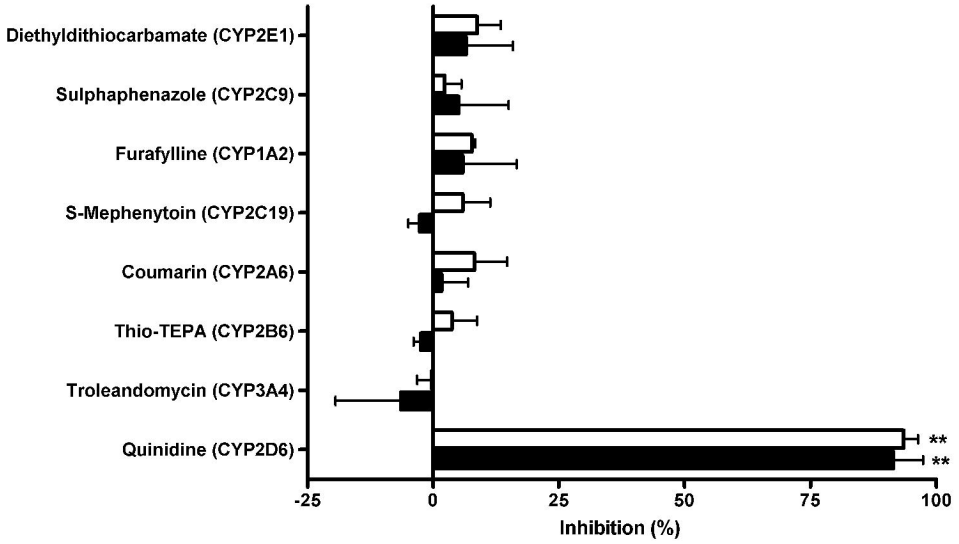

figure 5b

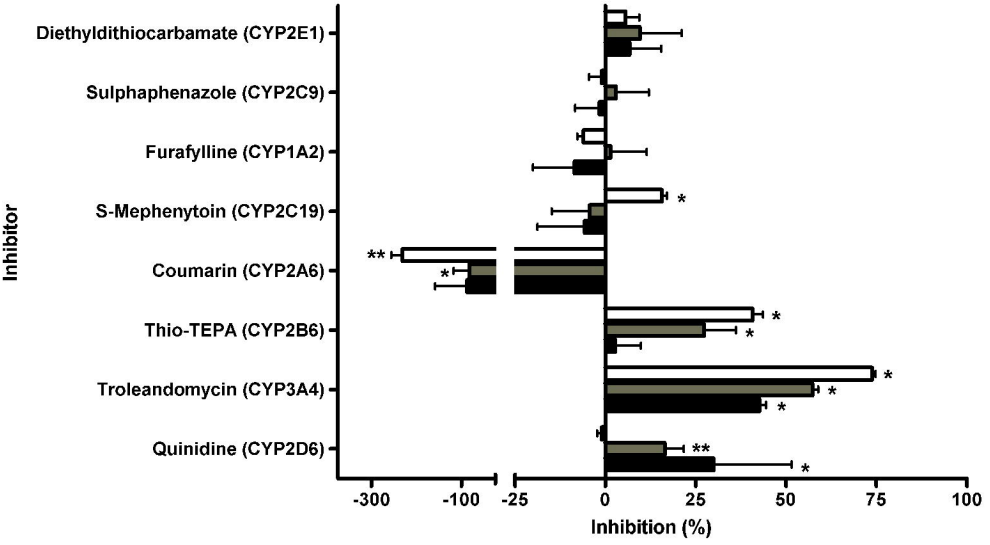

figure 5c

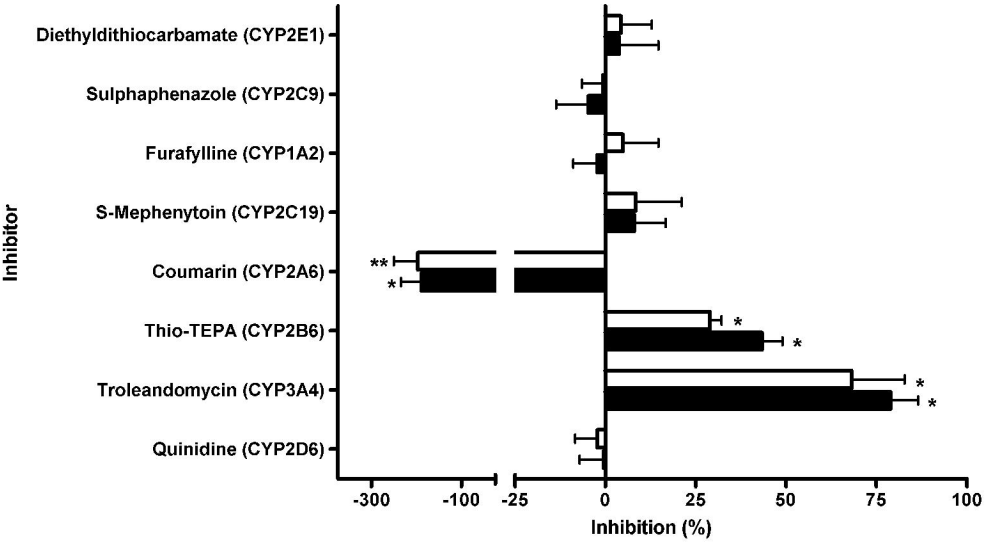

figure 6a

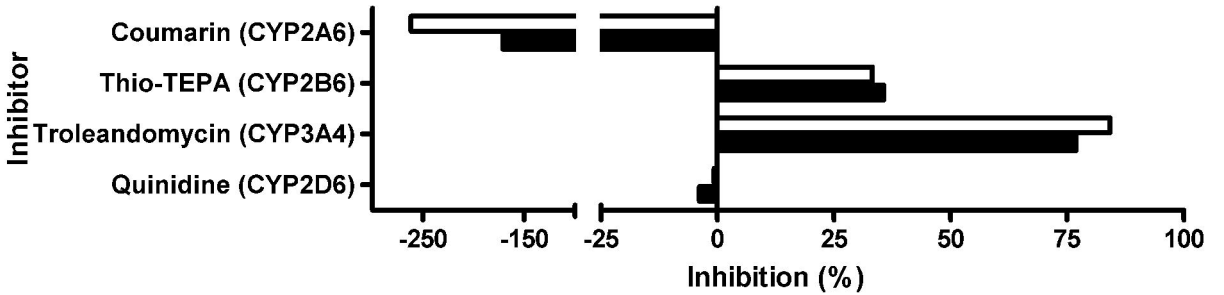

figure 6b

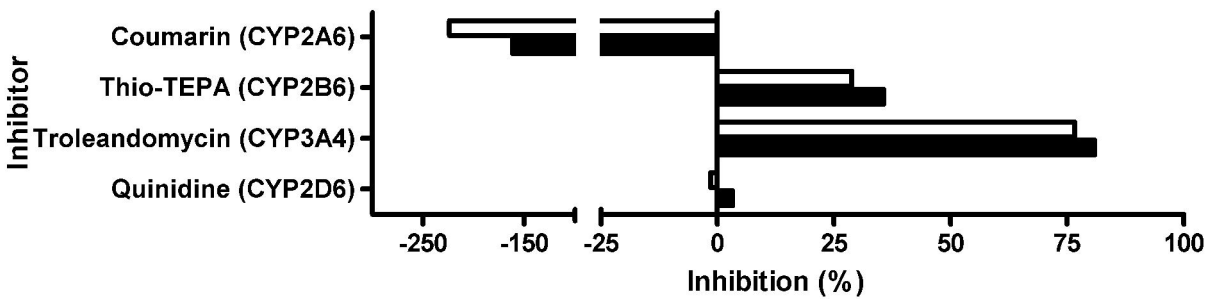

figure 7a

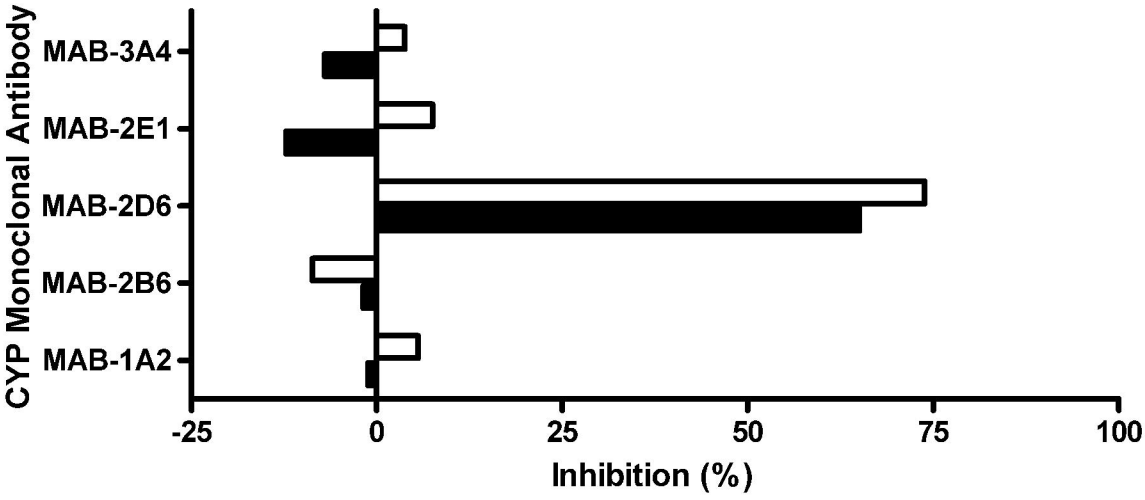

figure 7b

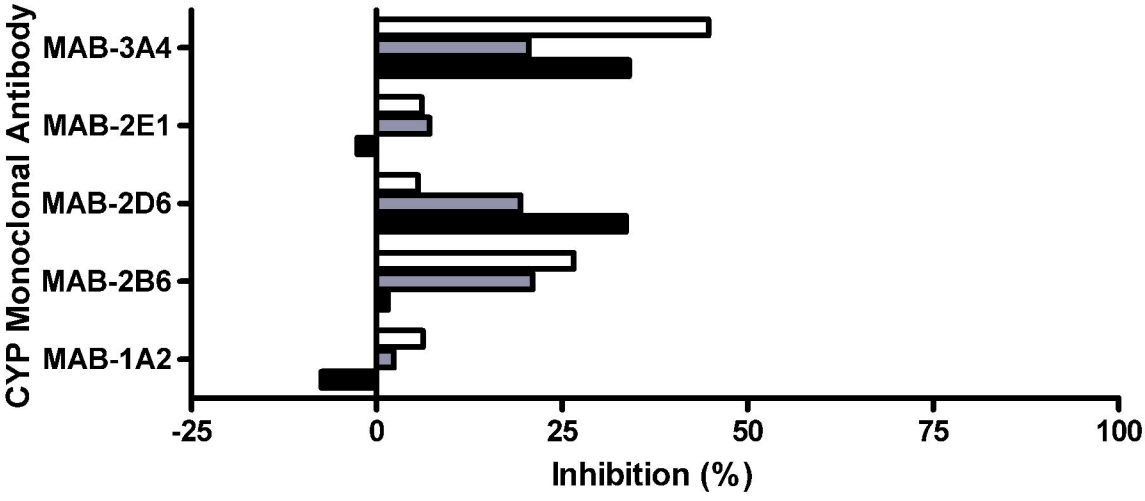

figure 7c

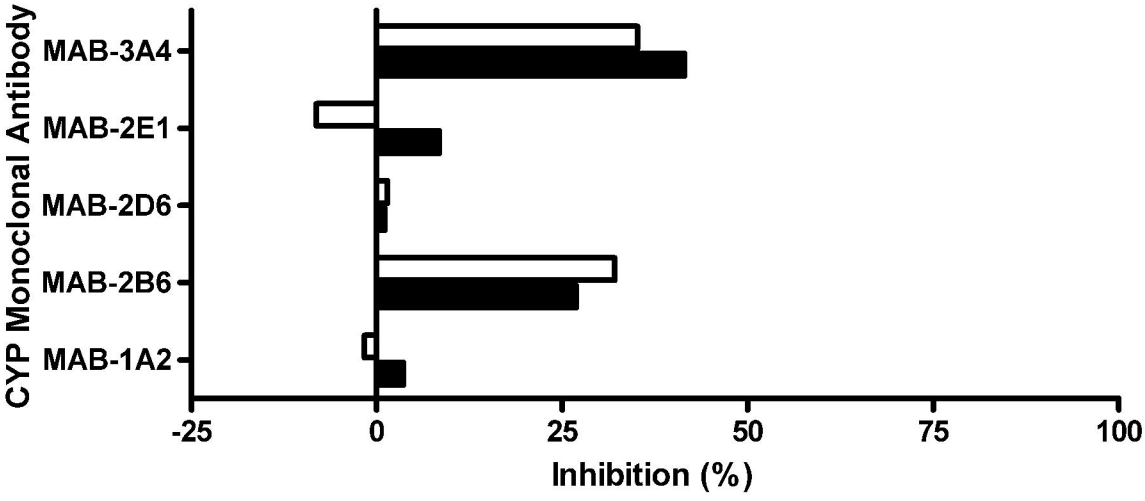

figure8a

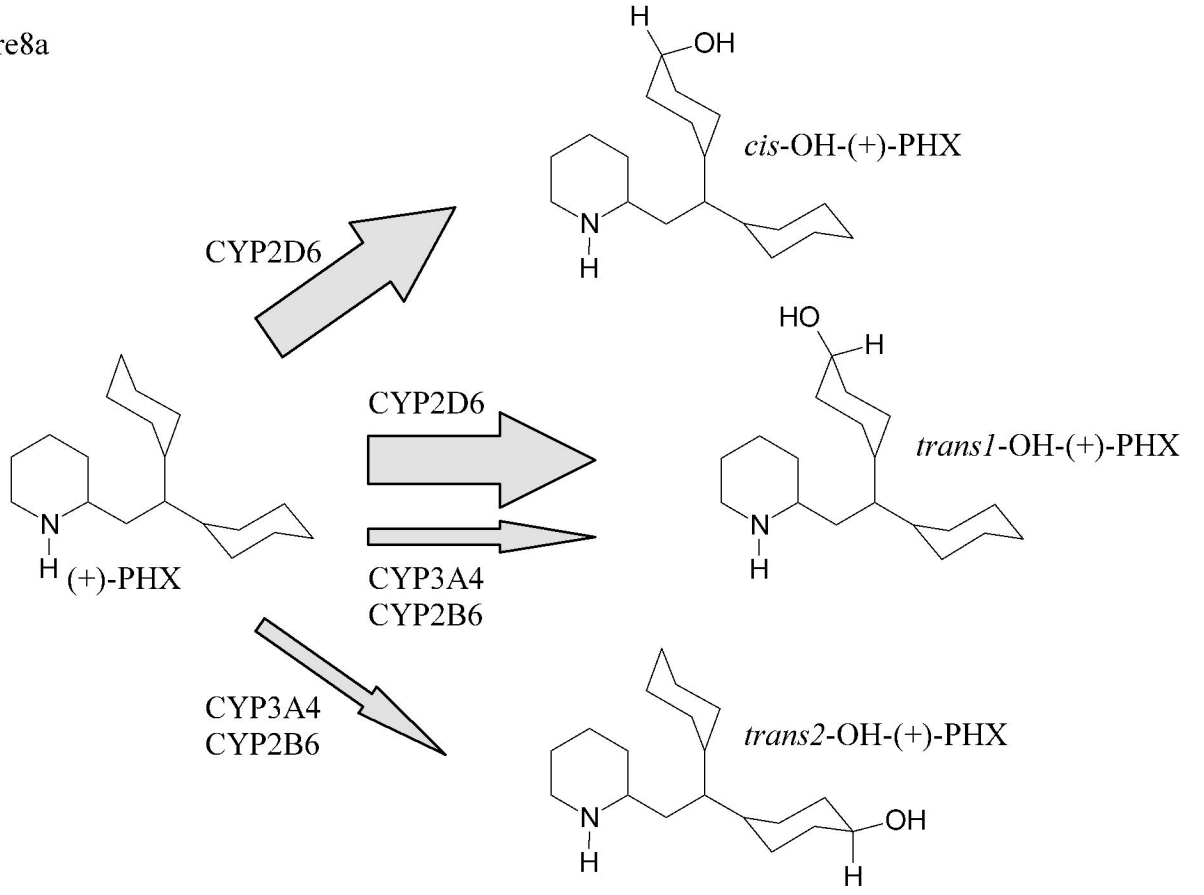

figure8b